Thin Silicon Nitride Metalens with long focal length for integrated optical sensors

D. De Vocht, T. Liu, K.A. Williams, Y. Jiao, and E.A.M. Bente

Photonic Integration Group, Department of Electrical Engineering, Eindhoven University of Technology, PO Box 513, 5600 MB Eindhoven, The Netherlands.
d.j.y.d.vocht@tue.nl

Abstract

We describe a metalens on an InP chip - with 455 nm tall SiN pillars on a silica layer and a diameter of 500 µm - that can produce a 100 µm wide spot at a distance of 12 mm. Such short SiN pillars cover a six times smaller phase shift range than required for an ideal lens. However, we experimentally demonstrate that it is possible to design a functioning metalens even with this reduced phase coverage. We designed and fabricated two SiN metalenses using cylindrical and cross-shaped pillars. They can focus a Gaussian beam up to a distance of 12.1 and 12.4 mm, respectively. We observe that the reduced phase shift leads to a doubling of the beam diameter at the focus as opposed to for an ideal lens. These lenses can be integrated into the InP Membrane on Silicon (IMOS) platform; combined with grating couplers they enable to realise e.g. optical sensors without additional components.

Metalenses are microscopically thin lenses composed of an array of nanopillars. By tailoring the shape of each nanopillar, the electrical field of the incoming beam can be controlled at each point in the array, allowing the manipulation of the overall amplitude and phase of the outcoming beam. To design the pillars, Silicon Nitride is particularly suited because it is transparent from the near-ultraviolet until the Near Infra-Red (NIR) [1]. SiN's refractive index is around 2 versus e.g. 3.45 for amorphous Silicon. But, for metalenses with low Numerical Aperture values (NA < 0.6) operating at a wavelength of 1550 nm, this difference of 1.45 does not lead to a considerable difference in performance [2]. In the visible regime, SiN metalenses exist which can achieve focusing efficiencies as high as 63 % and near-diffraction-limited focal spot sizes [3-4]. Using two metalenses varifocal tuning has been demonstrated reaching focal lengths up to 30 and 10 cm in the visible and NIR, respectively [5]. To achieve a full 2π phase shift, the pillars need to be taller than 0.695 and 1.55 µm for wavelengths of 633 nm and 1.55 µm respectively [2, 4]. However, fabricating such tall SiN pillars closely spaced to each other is challenging.
In this paper, we first investigate the phase coverage of 455 nm tall cylindrical and cross-shaped SiN pillars. We then design a SiN metalens that can produce an 85 µm spot at a distance of 12 mm (Fig. 1(a)). Afterwards, we present a process flow to fabricate them on an InP chip - a stepping stone to integration into the InP on Silicon Membrane (IMOS) platform. Finally, we analyze the performance of our fabricated metalenses.

Design

We use the 3D finite-difference time-domain method (FDTD) of Lumerical to calculate the transmission $T_m(\lambda)$ and phase $\varphi_m(\lambda)$ profile of cylindrical or cross-shaped SiN pillars on top of a SiO2 layer. Locally on the lens, we assume the pillars to have similar shapes and dimensions; therefore, we consider an infinitely periodic lattice. Figures 1(b-f) summarize the design parameters and show $T_m(\lambda)$ and $\varphi_m(\lambda)$ for both cylindrical and cross-shaped pillars. We notice no jumps in $T_m(\lambda)$ or $\varphi_m(\lambda)$. Thus, no resonances occur in the pillar as expected for the low pillar height. Both cylindrical and cross-shaped pillars only obtain a relatively small phase shift of 0.30π and 0.34π, respectively.

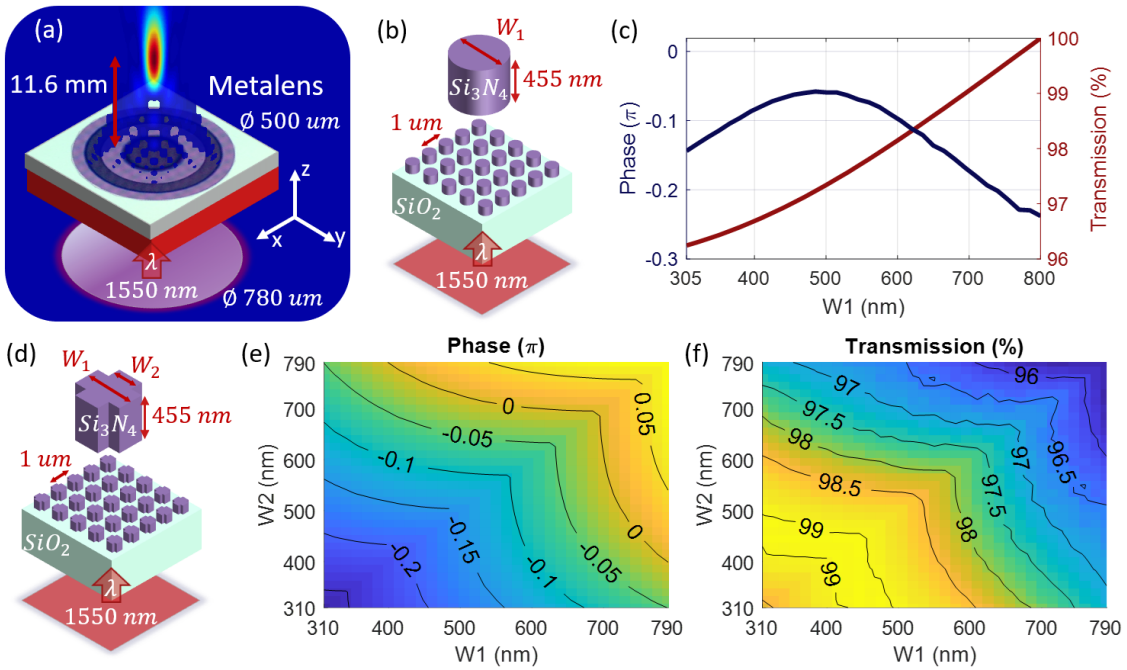

Fig. 1 (a) Overview of metalens' operation. **(b-f)** Schematic of the infinite cylindrical and cross-shaped arrays used in FDTD with its simulated transmission and phase profiles.

To focus a Gaussian beam at a focal length f, we require the following phase profile

$$\varphi(r,\lambda) = -\frac{2\pi}{\lambda}\left(\sqrt{r^2+f^2}\right) + C(\lambda) \qquad (1)$$

where r is the radial position, λ is the wavelength and $C(\lambda)$ is a spectral degree of freedom. Consequently, the metalens needs for our design parameters (Fig. 1(a)) a total phase shift of 3.45π, or relatively 2π. Thus, the SiN pillars possess a 6x smaller phase shift than ideally required. For each r, we identify the most optimal pillar m by minimizing the error between the desired and resulting electrical field near the lens plane

$$\min\left|\exp(i\,\varphi(r,\lambda)) - \sqrt{T_m(\lambda)}\,\exp(i\,\varphi_m(\lambda)\right| \qquad (2)$$

Since we cannot obtain full phase coverage, certain locations on the metalens have larger errors. Next, we calculate the far-field intensity of the metalens at $z = f$ according to the Rayleigh-Sommerfeld diffraction formula. Following this method, we design 2 SiN metalenses with cylinders (M1) and cross-shaped pillars (M2) that can produce a spot of 84 and 86 µm, respectively, whilst having $f = 11.6$ mm (Fig. 1(a)).

Fabrication

We fabricate the metalenses on a double-side polished InP wafer. First, we deposit a SiO_2 and SiN film of 2 µm and 455 nm thick, respectively, by plasma-enhanced chemical vapour deposition (PECVD) at 300 °C. We afterwards deposit a 50 nm-thick Cr mask using e-beam evaporation. To define the metalens pattern, we use a Raith EBPG5150 electron beam lithography tool on a 320 nm thick ZEP resist layer. After developing the resist, we transfer this pattern to the Cr mask by inductively coupled plasma (ICP) etching in a mixture of Cl_2 (15 sccm) and O_2 (15 sccm) at 60 °C with an ICP power of 500 W and an RF power of 5 W. Finally, we create the SiN pillars using a cyclic recipe of CHF_3 (100 ccm) reactive ion etching and O_2 (20 sccm) descum at an RF power of 50 W. We measure the etch selectivity between Cr and SiN to be around 20:1. Thus, the current etching process can theoretically etch up to 1000 nm for a 50 nm Cr mask. Though, mask erosion

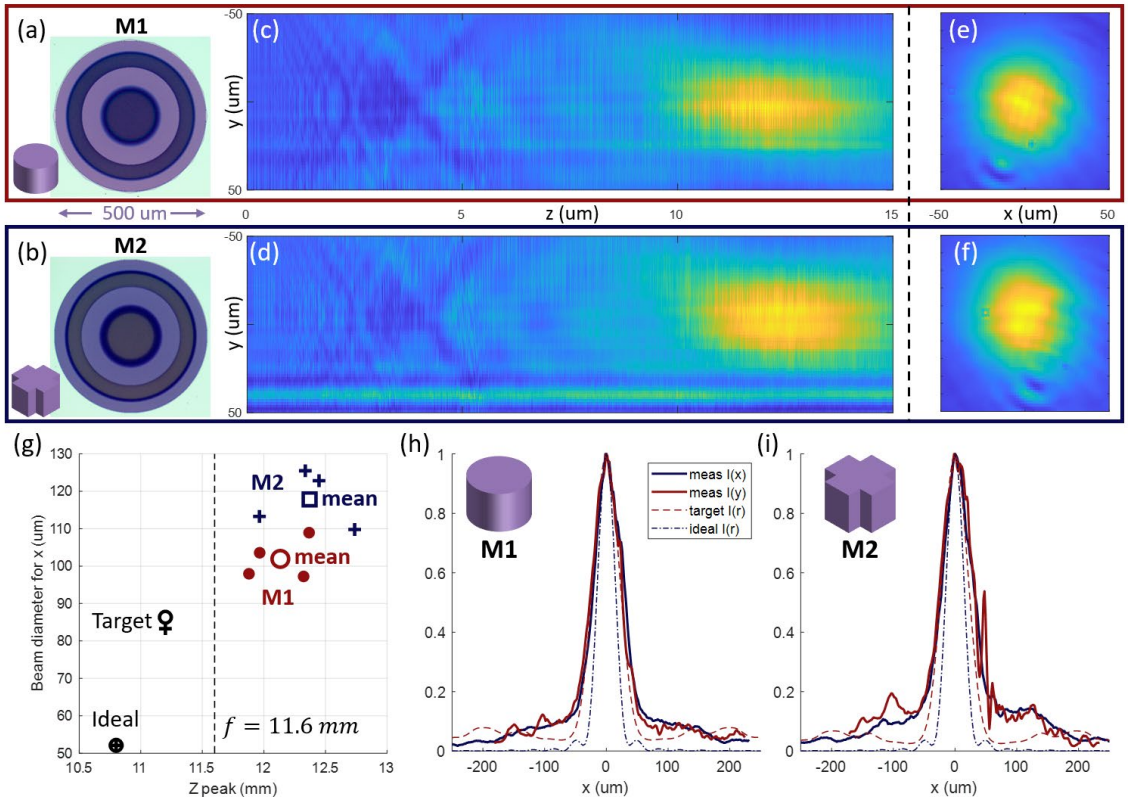

Fig. 2 (a-b) Optical image of metalens samples. **(c-f)** Measured far-field intensity distributions in the axial (yz cross-section) (**c-d)** and the focal plane (xy cross-section). **(h-i)** Horizontal (red solid) and vertical (blue solid) cuts across the measured focal spots and those of the simulated focal spots of the target (red dashed) and ideal (blue dashed) design **(g)** Calculated beam diameter (for x-direction) and location of maximum intensity for the measured samples M1 (red) and M2 (blue) - including their mean values - and for the simulated target and ideal lens design (black). **(a,c,e,g)** and **(b,d,f,h)** belong to the same sample of type M1 and M2, respectively.

in the lateral direction will limit the successful creation of such tall pillars.
Figures 2(a-b) present an optical image of a fabricated sample of types M1 and M2. We noticed that the pillar dimensions in the cross-section differ from the target design. This leads to a different phase shift at each target location. By compensating for this in the lithography step, we can obtain the correct pillar dimensions.

Performance

In the experimental set-up, we collimate a laser beam (CoBrite DX4 – ID Photonics) to obtain a Gaussian beam at a wavelength of 1550 nm with a beam diameter of 780 µm. After transmitting this beam through our metalens, we capture the light by a 20x microscope objective (Mitutoyo Plan APO NIR using a tube lens with a focal length of 200 mm) and image it onto an InGaAs camera (Xeva 320 - Xenics). We mounted the objective and the camera on a motorized stage (CONEX-MFACC - Newport) to measure the far-field at different distances.
We measured 4 samples of a metalens using cylinders (M1) and 4 of a metalens using cross-shaped pillars (M2). Figures 2(c-d) show the intensity distributions of 2 metalenses at different cross-sections. From the axial intensity distribution, we observe that the lenses

focus the Gaussian beam to a spot at a distance of 11.97 and 12.34 mm respectively. Figures 2(g-h) display the horizontal and vertical cuts of the measured focal spots and compare them with the simulation result of the target and ideal lens design. The ideal lens design exactly follows the phase profile of Eq. (1). Figure 2(i) shows the location of the peak intensity versus the beam diameter of our measured and simulated results. The extra beam in Figure 2(d), the narrow spots in Figures 2(e-f) and the extra peak in Figure 2(h) represent an artefact of the set-up because they are also present if we solely analyze the input beam.

Both metalenses M1 and M2 closely focus the light to the target focal length of 11.6 mm reaching on average a maximum peak intensity at z = 12.1 and 12.4 mm, respectively, whilst possessing similar peak intensities (measured to differ only 1.2 %). We notice that the ideal and target design reach their peak intensity at a smaller value due to diffraction of the beam (Fig. 2(i)). The beam diameter of the target design is 1.7x (M1) and 1.6x (M2) larger than the ideal lens as can be explained due to the lower phase shift range. On average, the beam diameter of the measured samples is 2.0x (M1) and 2.3x (M2) larger than the ideal case. Fabrication defects cause this extra broadening. The intensity distribution of the target and ideal design present sidelobes because the input's beam diameter is 1.6x larger than the metalens' diameter (Fig. 1(a) and 2(g-h)). Using a stronger collimator, we expect to measure more intensity in the main lobe.

Conclusion

We calculate that using 455 nm high SiN pillars a limited range of phase shifts can be realised of approx. $2\pi/6$ at a wavelength of 1550 nm. However, after designing and fabricating samples, we demonstrated that for an NA of 0.022 it is possible to create a functioning metalens even with this reduced phase shift range. We notice a similar performance for thin SiN metalenses using cylindrical and cross-shaped pillars. Both lenses can focus the light to a distance only 0.5 and 0.8 mm further than the desired focal length, respectively. Due to the limited phase shift range, their beam diameter is twice large as compared to an ideal lens. To characterize the full behaviour of the metalens, we will analyze their focusing efficiency and phase front. These lenses can be integrated into the IMOS platform; combined with grating couplers they enable to realise e.g. optical sensors without additional components.

Acknowledgements

This publication is part of the project FreeSense with project number 17971 of the research program HTSM which is financed by the Dutch Research Council (NWO). We thank Irwan Setija for the insightful discussions.

References

[1] S. Colburn *et al.*, "Broadband transparent and CMOS-compatible flat optics with silicon nitride metasurfaces [Invited]," *Optical Materials Express, Vol. 8, Issue 8, pp. 2330-2344*, Aug. 2018.

[2] E. Bayati *et al*, "Role of refractive index in metalens performance," *Applied Optics, Vol. 58, Issue 6, pp. 1460-1466*, Feb. 2019.

[3] S. Colburn *et al*, "Metasurface optics for full-color computational imaging," *Science Advances, Vol. 4, Issue 2,* Feb. 2018.

[4] Z.-B. Fan *et al.*, "Silicon nitride metalenses for unpolarized high-NA visible imaging," *Conference on Lasers and Electro-Optics*, May 2018.

[5] S. Colburn *et al*, "Varifocal zoom imaging with large area focal length adjustable metalenses," *Optica, Vol. 5, Issue 7, pp. 825-831*, pp. 825–831, Jul. 2018.